Electronic Supplementary Information

Uncovering divergent evolution of α/β-hydrolases: a surprising residue substitution needed to convert *Hevea brasiliensis* hydroxynitrile lyase into an esterase

David M. Nedrud, Hui Lin, Gilsinia Lopez, Santosh K. Padhi, Graig A. Legatt, Romas J. Kazlauskas

University of Minnesota, Department of Biochemistry, Molecular Biology & Biophysics and The Biotechnology Institute, 1479 Gortner Avenue, Saint Paul, MN 55108 USA

Contents

Sequence alignments

Alignment of the amino acid sequences of of two HNLs and two esterases using Clustal O[1] shows a conserved Ser-His-Asp catalytic triad in both groups, as well as many identical and similar residues, Figure S1. Purple highlights the three active site residues chosen for mutagenesis to convert *Hb*HNL into an esterase.

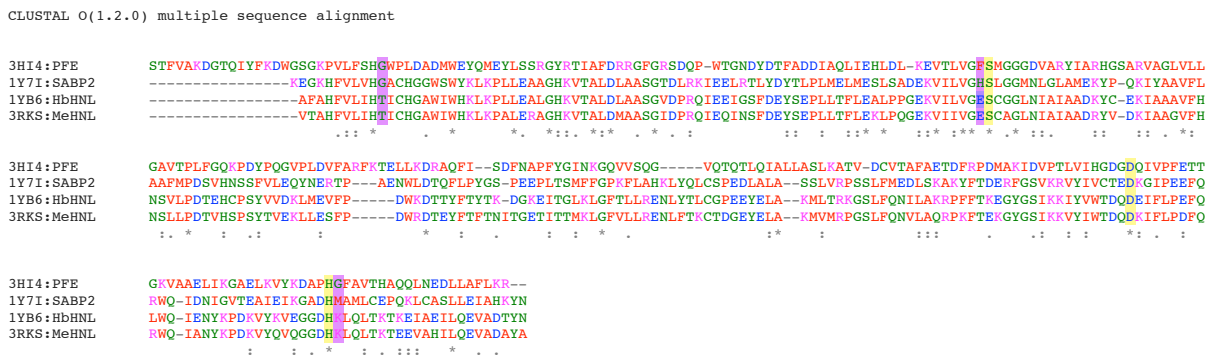

Figure S1. Multiple sequence alignment (Clustal O) of *Hevea brasiliensis* HNL, *Manihot esculenta* HNL, *Pseudomonas fluorescens* esterase, and salicylic acid binding protein (esterase). Yellow highlights show the conserved Ser-His-Asp residues of the catalytic triad; purple highlights three active site residues chosen to convert *Hb*HNL into an esterase. At residue 236 of HbHNL the esterases contain either a Gly or Met. Both possible substitutions were tested. The letter colors indicates the type of amino acid: red for hydrophobic, green for hydrophilic, magenta for basic, and blue for acidic. Below the letters, the . represents a location having similar amino acids, the : represents highly conserved residues, and the * represents identical amino acids.

The rationale for choosing these three residues come from an overlay of the x-ray crystal structures of SABP2 and *Hb*HNL and the extensive kinetic and mechanistic work by the Griengl and Kratky groups. A comparison of the active site of *Hb*HNL with the modeled active site of the variant, *Hb*HNL-TM, shows the changes in the active site, Figure S2A & B. The substitutions increase the space near the catalytic serine residue and allow access to the oxyanion hole.

A phylogenetic tree of α/β-hydrolases,[2] shows that *Hb*HNL and SABP2 had a common ancestor that may have one or both catalytic activities.

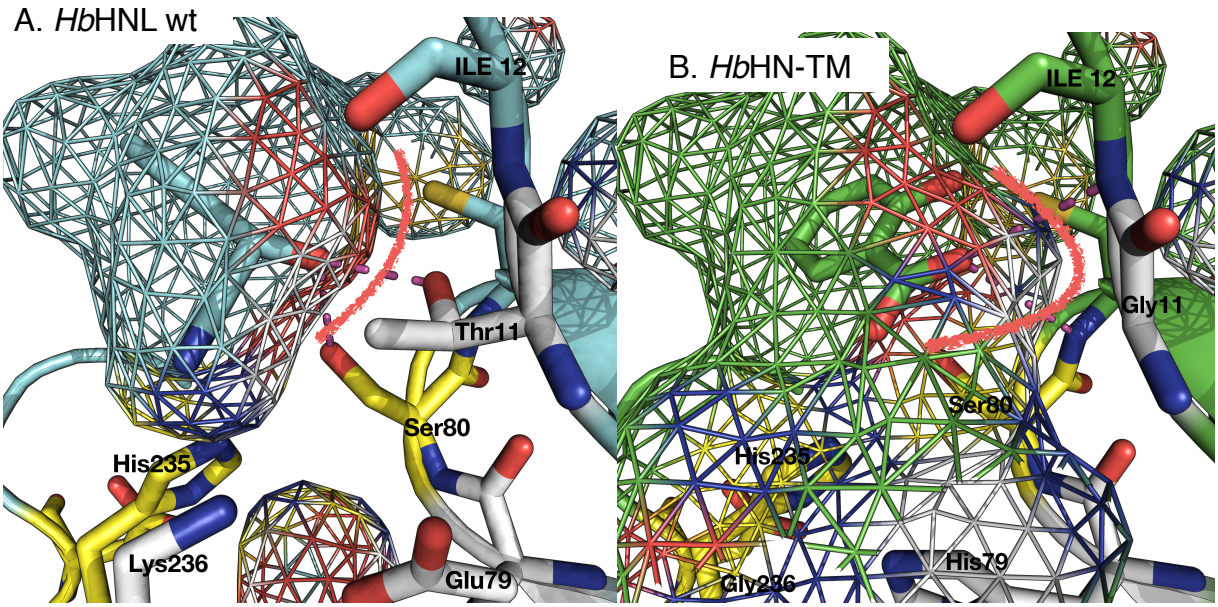

Figure S2. Active sites of *Hb*HNL and *Hb*HNL-TM variant and phylogenetic tree of α/β-hydrolases. (A) Active site from a crystal structure of *Hb*HNL wt containing bound mandelonitrile (pdb code: 1YB6). Grey residues indicate the sites for substitution and the mesh outlines the space available for the substrate as detected by the space available for a 3-Å diameter sphere, which mimics a water molecule. (B) Model of the active site of *Hb*HNL-TM variant (*Hb*HNL Thr11Gly Glu79His Met236Gly) illustrates the increased space available for the substrate and an optimized orientation for salicylic acid. The most important expansion is the creation of an oxyanion hole shown by the red line. Figures A and B were created using the visualization software PyMOL (www.pymol.org)

Protein purification

The cell lysates containing *Hb*HNL and its variants were separated using a High Q anion exchange column (Biorad). Proteins were eluted with buffer (50 mM Tris pH 7.5) with stepwise increases in NaCl concentration. The fraction with the purest target protein, which eluted with 130 mM NaCl for the example in Figure S3, was concentrated to 500 μL and further purified on a Sephadex G75 gel filtration column (150 mL, GE Healthcare) equilibrated with phosphate buffer (50 mM, pH 7.5 containing 300 mM NaCl). The column was eluted at 0.5 mL/min while collecting 1 mL fractions. Conductivity averaged 25 mS/cm and showed a sharp symmetrical peak for the target protein and a leading shoulder that contains impurities. The fractions containing pure target protein were pooled. The buffer was exchanged by concentrating using an centrifuge tube with an ultrafiltration membrane and diluting the concentrated solution 100 fold with BES buffer (20 mM, pH 7.2) before characterization, Figure S4. Purity was verified by SDS PAGE. The gels in Figures S3-4 are the purification of *Hb*HNL Thr11Gly Glu79Gly Lys236Gly (*Hb*HNL TM). When calculating catalytic activity, samples were assumed to be homogenous, so the activities are a lower limit.

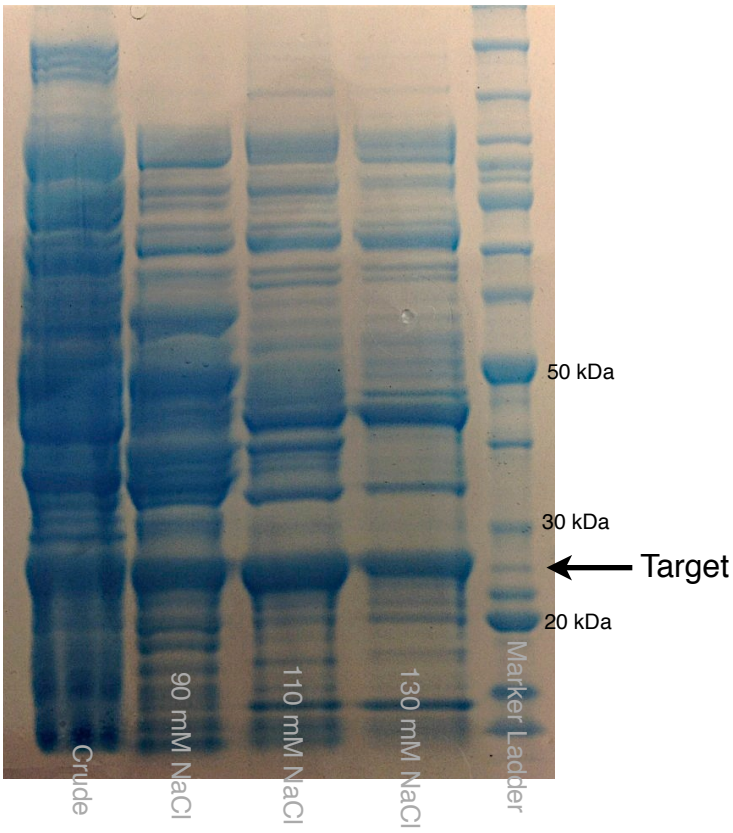

Figure S3. SDS-PAGE of the fractions eluted during anion exchange chromatography of *Hb*-HNL-TM. Proteins were eluted with the stepwise increases in sodium chloride concentrations shown. The protein fraction that eluted with 130 mM NaCl was further purified by gel filtration chromatography. Nu PAGE 4-12% bis-tris gel

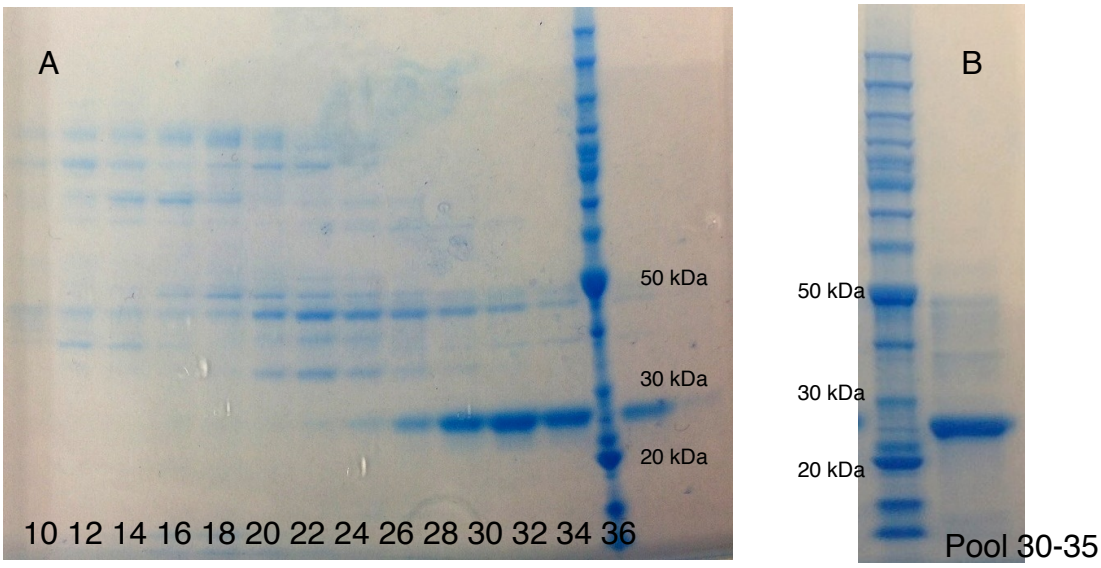

Figure S4. SDS-PAGE of fractions eluted during gel filtration chromatography of *Hb*HNL TM and final purity. (A) Fractions eluted during gel filtration of *Hb*HNL TM. Fractions 30-35 were

pooled and characterized. (B) One μg of the final purified sample of *Hb*HNL TM; this is typical of all variants. Nu PAGE 4-12% bis-tris gel

Native-gel electrophoresis stained with an esterase-specific stain[3] identified the protein responsible for the low background esterase activity in *E. coli* BL21 lysate. Native gel electrophoresis of lysate from BL21 grown using the standard protein expression procedure and several control proteins was stained with both Commassie blue to show all proteins and esterase to show proteins with esters activity, Figure S6 A. Esterase staining solution contained 100 mM Tris, pH 7.5,2-napthyl acetate (0.1 g in 1 mL ethanol), and Fast Blue RR diazonium salt (1 mL). This diazonium salt was prepared by dissolving Fast Blue (2 g) in 1 M HCl (10 mL), cooling in an ice bath and slowly adding sodium nitrite (2 g) while keeping the temperature ≥5 ˚C. The gel was covered with staining solution for 20 mins and then washed in 30% methanol for 20 mins. Two bands showed esterase activity; these were cut out from the gel and protein was extracted with 50% acetonitrile and 50 mM Tris buffer pH 7.5. The positive control of SABP2 confirmed the reaction worked and the negative control of HbHNL wt confirmed our purification method removed the contaminating esterase. The extracted protein was concentrated and heated in sodium dodecyl sulfate sample buffer for visualization of protein size by SDS-PAGE gel, Figure S5B. The SDS-PAGE gel showed only one band at 17 kDa and this band has been removed from the *Hb*HNL purified protein sample.

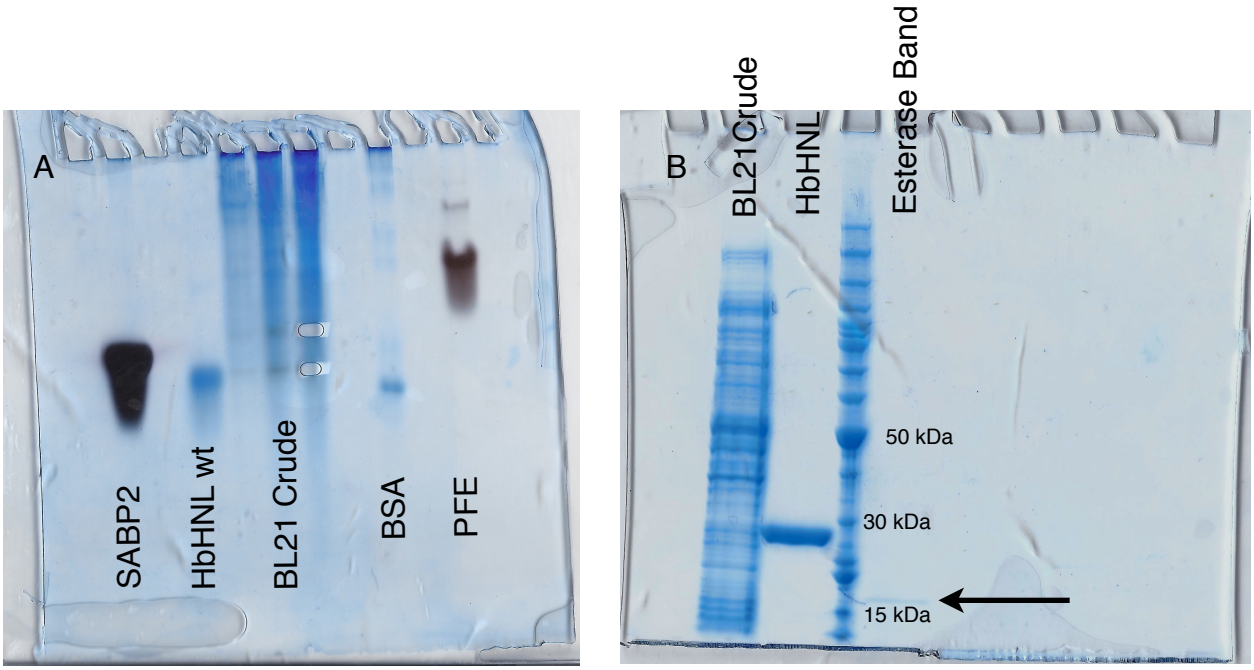

Figure S5. Gel electrophoresis to identify the contaminating esterase in *E. coli* BL21. **A:** Native polyacrylamide stained with both esterase stain (dark purple) to show proteins with esterase activity and Commassie (blue) to show all proteins. The three lanes near the BL21 crude label contain increasing amounts of crude lysate protein. SABP2 and PFE served as positive controls, while wt HbHNL and bovine serum albumin (BSA) served as negative controls. The 8-12% trisgly gel was run at a constant current of 25 mAmps for 3.5 h. **B:** SDS-PAGE of the proteins cut from lane 4 and HbHNL wt in lane 2 of the native gel in panel A. Lane 1 contained crude protein

and lane 3 contains Invitrogen benchmark protein ladder. The contaminating esterase runs at an apparent molecular weight of ~17 kDa.

The 17 kDa protein was extracted from the gel, digested with trypsin and resulting peptides sequenced by LC-MS. The mass spectra were compared using Sequest (Thermo Fisher Scientific, v. 27, rev. 12) with the *Escherichia coli* protein database (rs_ecoli_v201004_cRAP containing 270,265 entries) with a fragment ion mass tolerance of 0.80 Da and a parent ion tolerance of 1.00 Da, iodoacetamide derivative of cysteine as a fixed modification and oxidation of methionine as a variable modification. The best match was alkyl hydroperoxide reductase C22 (GenBank: AAB40806.1), which matched 13 unique peptides, 15 unique spectra, 27 total spectra, 149/187 amino acids (80% coverage). The molecular weight of alkyl hydroperoxide reductase (20.8 kDa) is close to the 17 kDa seen in the gel. The active site of this reductase contains a nucleophilic cysteine; it is conceivable that this reductase may catalyze promiscuous ester hydrolysis, but this activity has not been previously reported.

MSLINTKIKP FKNQAFKNGE FIEITEKDTE GRWSVFFFYP ADFTFVCPTE
LGDVADHYEE LQKLGVDVYA VSTDTHFTHK AWHSSSETIA KIKYAMIGDP
TGALTRNFDN MREDEGLADR ATFVVDPQGI IQAIEVTAEG IGRDASDLLR
KIKAAQYVAS HPGEVCPAKW KEGEATLAPS LDLVGKI

Figure S6. Alkyl hydroperoxide reductase C22's amino acid sequence matched best to the sequences of peptides from a trypsin digest of the protein with esterase activity. Yellow highlights the amino acids matched in the peptides.

Steady state kinetics & additivity of the effects of mutations

The esterase and hydroxynitrile lyase activities were measured by spectrophotometrically using *p*-nitrophenyl acetate (monitored at 404 nm) and mandelonitrile (monitored at 280 nm), respectively, as substrates, Figure S7, as described in the experimental section. Calculations assume that the protein was pure, so they underestimate the catalytic activity for impure proteins.

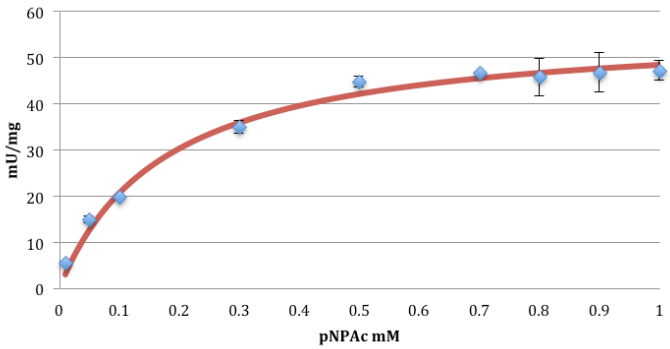

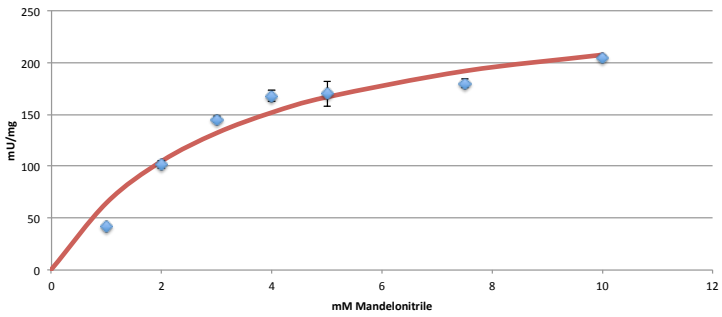

Figure S7. Michaelis-Menten curves for the variant *Hb*HNL Thr11Gly-Lys236Gly-Glu79His for (A) esterase activity for hydrolysis of *p*-nitrophenyl acetate (k_{cat} = 1.62 min^{-1}; K_m = 0.16 mM) and (B) HNL activity for cleavage of mandelonitrile (k_{cat} = 8.1 min^{-1}; K_m = 3.2 mM). Kinetic constants were determined by nonlinear fit to the equation $V_o=V_{max}[S]/([S]+K_m)$. These data are typical of that used to determine kinetic constants.

A summary of the steady state kinetic data for all variants, Figure S8, shows that combining substitutions often increased catalytic activity synergistically, that is, by more than the sum of the individual substitutions. There was no obvious trend for the values of k_{cat} and K_m, but the k_{cat}/K_m steadily increased with increasing numbers of substitutions. This increase shows that each substitution contributes to esterase activity. These contributions are not additive because the activity for the triple substitution is much greater than the sum of the activities for the three single substitutions.

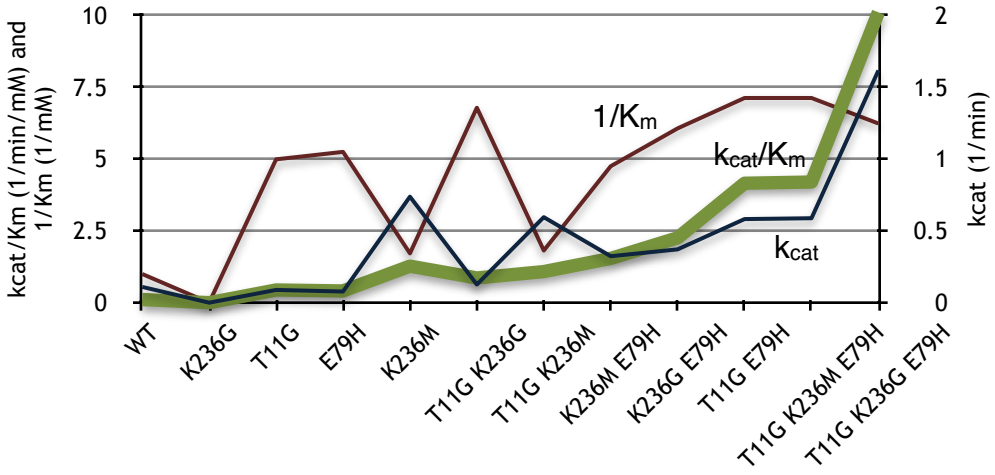

Figure S8. Steady state kinetic constants for hydrolysis of *p*-nitrophenyl acetate catalyzed by *Hb*HNL variants. The values of k_{cat} (black line) use the right y-axis, while k_{cat}/K_m (green) and $1/K_m$ (red) use the left y-axis. Esterase activity increases non additively as seen by k_{cat}/K_M values for the triple-substitution variants being much higher than the sum of the corresponding three single substitution variants. The single substitution variant *Hb*HNL K236G did not yield soluble protein, so its catalytic activity could not be measured. Its k_{cat} and k_{cat}/K_M values are shown as zero.

pH dependence of esterase activity of *Hb*HNL-TM

Electrostatic effects of the Glu79His substitution were measured by the change in pH dependence of pNPAc hydrolysis catalyzed by *Hb*HNL Thr11Gly Lys236Gly and *Hb*HNL Thr11Gly Lys236Gly Glu79His. First, the extinction coefficients of p-nitrophenol was measured at different pH, Figure S9.

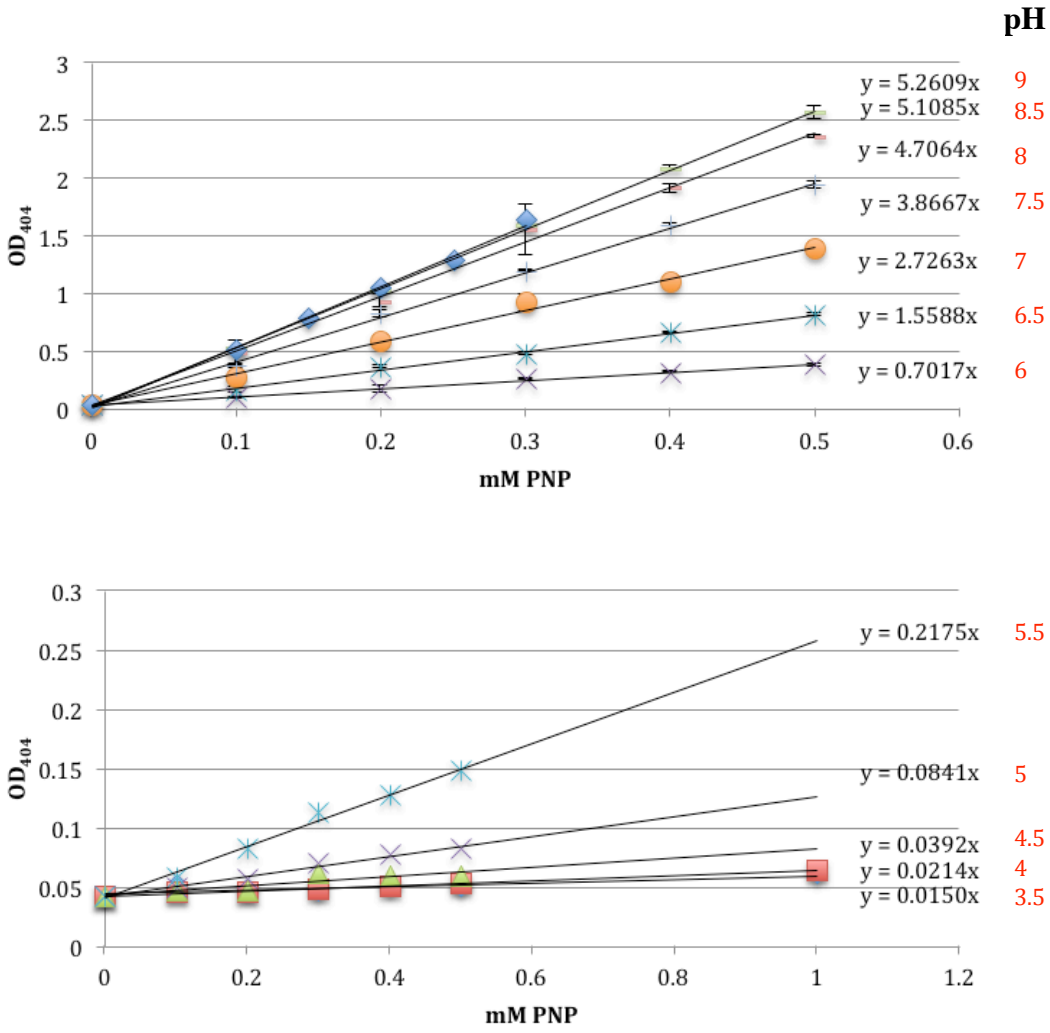

Figure S9. Measurement of extinction coefficient at 404 nm (OD_{404}/mM PNP) of *p*-nitrophenol in 6.7 vol% acetonitrile at different pH. The following buffers (20 mM) were used: citrate (pH 3.5 to 6.0), BES (pH 6.5 to 7.5), and Tris HCl (pH 8.0 to 9.0). These extinction coefficients were used to measure the amount of *p*-nitrophenol released from the hydrolysis of *p*-nitrophenyl acetate at different pH.

The relative activity as a function of pH identifies the kinetic pK_a for ester hydrolysis, Figure S9. This value corresponds the pK_a of the catalytic histidine in its catalytic form. The kinetic pK_a

with the Glu79His substitution (6.0) is similar to that without the substitution (5.8), indicating that the glutamate does not significantly alter the pK_a of the catalytically active form.

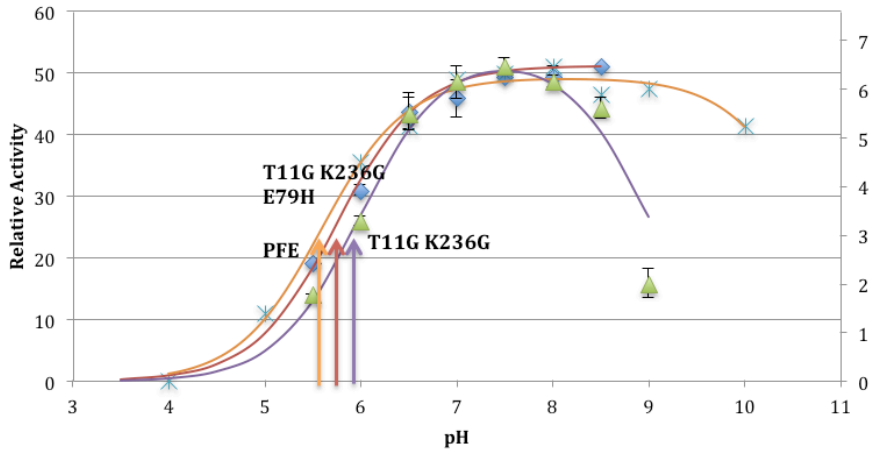

Figure S9. pH dependence of pNPAc hydrolysis by *Hb*HNL variants with and without the Glu79His substitution. The kinetic pK_a of esterase activity for the variants occurs at 6.0 and 5.8, respectively and at pH 5.6 for the esterase from *Pseudomonas fluorescens*. The assays were buffered with 20 mM citrate from pH 3.5 – 6, BES pH 6.5 – 7.5, and Tris pH 8 – 9. The assay mixture contained pNPAc (1 mM, approx. 5 x K_M of the *Hb*HNL variants) and 6.7 vol% acetonitrile. Data for PFE are from reference 4.

Hydrolysis of unactivated esters by *Hb*HNL TM and of natural substrates by wt and TM

To measure esterase activity toward other substrates besides pNPAc, we used a pH indicator, p-nitrophenol, to measure release of acid upon hydrolysis of the ester. Acid release protonates the phenoxide causing a decrease in absorbance at 404 nm. Figure S10 through S12 show the Michaelis Menten kinetics for a variety of esters using pH indicators. Figure S13 shows steady state kinetics for cleavage of cyanohydrins.

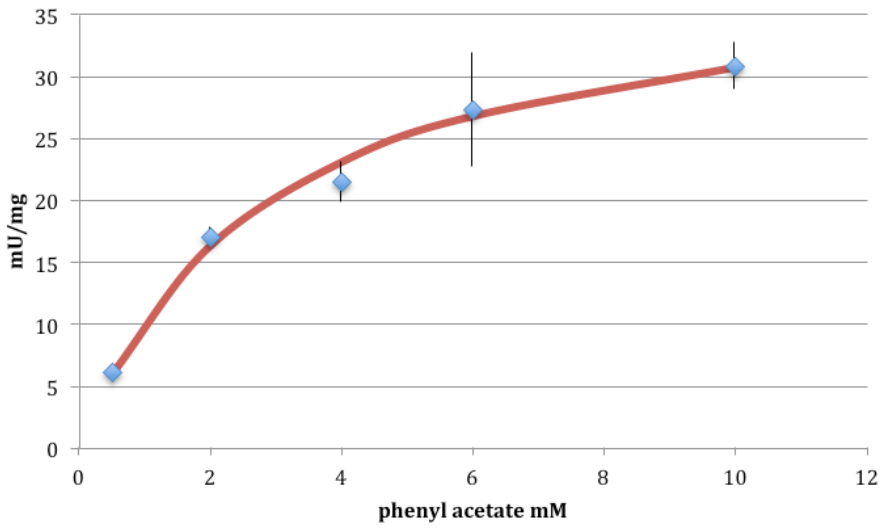

Figure S10. Steady state kinetics for the hydrolysis of phenyl acetate catalyzed by *Hb*HNL TM. Release of acetic acid at pH 7.2 was measured with *p*-nitrophenol as the pH indicator. These data yield values of k_{cat} = 1.2 min^{-1} and K_m = 2.8 mM.

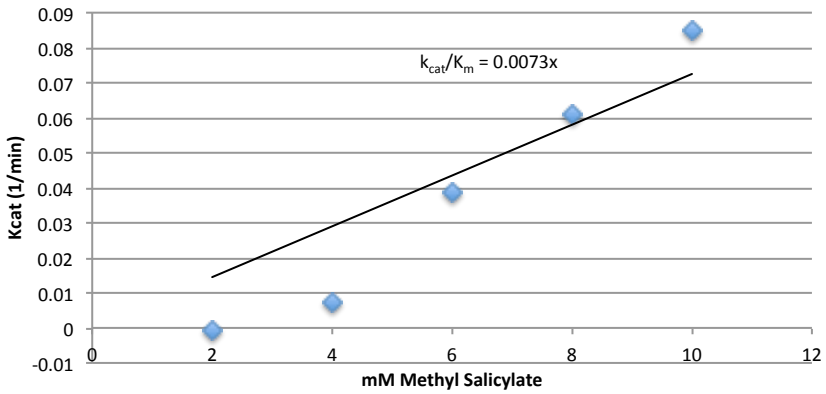

Figure S11. Hydrolysis of methyl salicylate by *Hb*HNL TM and detection of the product, salicylic acid, by a pH indicator. Initial slope was used to determine k_{cat}/K_m. Individual constants were estimated based upon limits of solubility; k_{cat} is greater than 0.1 min^{-1} and K_m is greater than 10 mM.

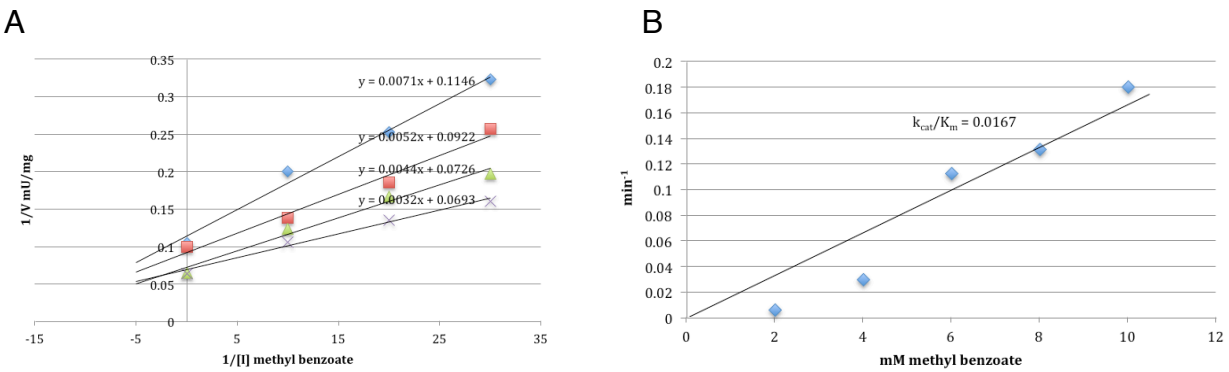

Figure S12. Hydrolysis of methyl benzoate by *Hb*HNL TM and kinetic constants determined by initial slope and inhibition constant. (A) The binding of methyl benzoate to HbHNL-TM was measured by the competitive inhibition of pNPAc hydrolysis activity by methyl benzoate yielded 9.2 mM for the inhibition constant. (B) The initial slope of a plot or reaction rate at increasing substrate concentration yields the value of k_{cat}/K_m. If we assume that Km is 9.2 mM, then we estimate that k_{cat} is 0.15 min^{-1}.

The natural substrate for *Hb*HNL, acetone cyanohydrin, is smaller than mandelonitrile and lacks the phenyl ring. The catalytic activity of *Hb*HNL-TM was much lower than for wild type. The value of k_{cat} dropped and the binding strength decreased (K_m increased). This decrease in catalytic activity was larger than for mandelonitrile.

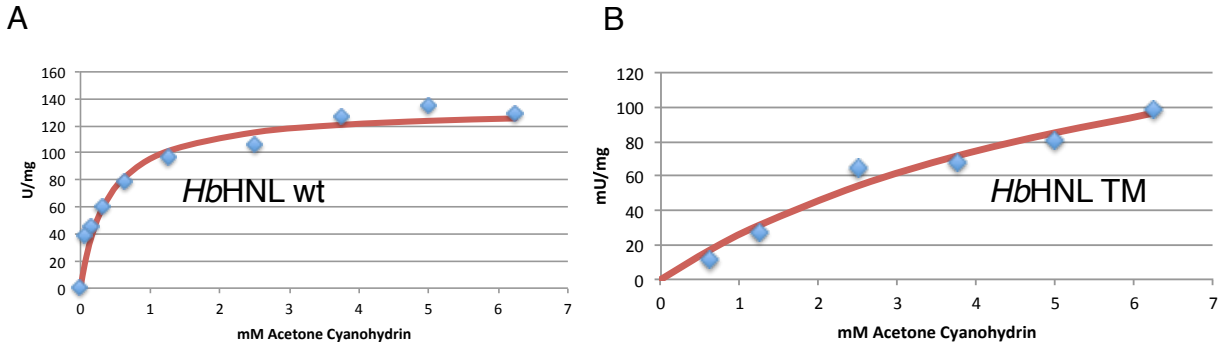

Figure S13. Steady state kinetics for the cleavage of acetone cyanohydrin catalyzed by HbHNL. (A) *Hb*HNL wt K_m and k_{cat} were 0.4 mM and 3900 min^{-1}. (B) *Hb*HNL TM K_m and k_{cat} were 6.5 mM and 5.8 min^{-1}. Acetone cyanohydrin cleavage was measured by the release of cyanide at 2, 5, and 10 mins and fit to a straight line.

References

1 F. Sievers, A. Wilm, D. Dineen, T. J. Gibson, K. Karplus, W. Li, R. Lopez, H. McWilliam, M. Remmert, J. Söding, J. D. Thompson, D. G. Higgins, *Mol. Systems Biol.* 2011, *7*, 539.

2 M. E. Auldridge, Y. Guo, M. B. Austin, J. Ramsey, E. Fridman, E. Pichersky, J. P. Noel, *Plant Cell* **2012**, *24*, 1596–1607; see supplemental material Figure S3.

3 N. Thangthaeng, N. Sumien, M. J. Forster, R. A. Shah, L.-J. Yan, *J. Chromatogr. B Analyt. Technol. Biomed. Life Sci*. 2011, *879*, 386–394.

4 N. Krebsfanger, F. Zocher, J. Altenbuchner, U. T. Bornscheuer, *Enzyme Microb. Tech*. 1998, *22*, 641–646.